33RD CONGRESS
OF THE INTERNATIONAL COUNCIL
OF THE AERONAUTICAL SCIENCES
STOCKHOLM, SWEDEN, 4-9 SEPTEMBER, 2022

ICAS 2022 SWEDEN

ASSESSMENT OF A SERIAL COOLING CONCEPT FOR HTPEM FUEL CELL SYSTEMS FOR AVIATION APPLICATIONS

Antje Link[1], Jonas Ludowicy[1] & Martin Staggat[1]

[1]German Aerospace Center (DLR), Institute of Electrified Aero Engines, Cottbus, Germany

Abstract

The thermal management subsystem is a significant mass contributor to a fuel cell system. In this paper a serial cooling concept for high temperature proton exchange membrane fuel cell systems is introduced and analysed. For a liquid cooling system, the coolant mass has a high share of the overall thermal management system mass. A cooling concept where multiple fuel cell units are put in serial from a coolant flow perspective allows for an increase in total temperature difference over the coolant and therefore significant reduction of coolant mass. As the temperature difference over each fuel cell unit is kept constant at 10 K, the different fuel cell units operate at different temperatures. This results in slightly less efficient and heavier fuel cell units. Furthermore, the increased overall temperature difference of the coolant also has an impact on the heat exchanger design. These trade-offs are evaluated for a different number of fuel cell units in serial and different design parameter combinations. The studies indicate that the proposed serial cooling concept offers significant weight savings or efficiency improvements, which can be traded against each other.

Keywords: fuel cell, HTPEMFC, thermal management strategy, serial cooling concept, electric propulsion

1. Introduction

To reduce the impact of aviation on climate, significant reductions in greenhouse gas emissions were set as goals in the Flightpath 2050 strategy paper [1]. According to this paper, the CO_2 emissions of aircraft have to be reduced by 75 % compared to the reference year 2000. For the next generation of aircraft, this results in a need for new and revolutionary propulsion technologies. Electric propulsion is a possible technology that enables such ambitious reductions in greenhouse gas emissions. Albeit the first fully-electric aircraft are flying [2], it remains challenging to bring fully-electric propulsion concepts to larger commercial passenger transport aircraft. While advances in battery technology can be expected to increase the options of small-scale electric applications in the near future, electrification of larger aircraft propulsion systems will only be possible via alternative energy sources in the foreseeable future [3].

An alternative means of energy storage is hydrogen. Hydrogen can be produced climate neutral from green electricity and offers the opportunity to completely eliminate all greenhouse gas emissions, except water vapour and contrails [4]. On one hand it could be used as a substitute for fossil fuel in a turboprop or turbofan engine, on the other hand it could be converted into electricity using a fuel cell and therefore enable the additional benefits of electric propulsion, such as highly efficient powertrains, lower noise emissions, or distributed propulsion concepts [5, 6].

While storage and conditioning of hydrogen comes with its own new set of challenges the focus of the present paper is on the thermal management of high temperature proton exchange membrane fuel cells (HTPEMFC). Since these types of fuel cells reach efficiencies of 30 to 60 % they produce a large amount of heat during operation. The relatively small mass flows through a fuel cell are not sufficient to carry all of this heat away. Therefore, an additional heat sink realised by an active thermal management system (TMS) is required for higher power classes. This subsystem introduces additional mass and a parasitic power loss [7].

There are different cooling concepts available for proton exchange membrane fuel cell (PEMFC) systems. They are designed to maintain the fuel cells operating temperature as well as to provide a very uniform temperature distribution over each cell for stable operation and longevity [7]. The available cooling methods range from air cooled to liquid cooled to phase change based systems. For higher power classes (>10 kW), usually liquid cooling systems are employed [8, 9] with phase change based systems as an alternative. The heat pick-up can either be achieved via internal cooling channels inside the fuel cell stacks or externally by heat spreaders [10, 11].
For larger aircraft, low temperature proton exchange membrane fuel cells (LTPEMFC) based propulsion systems have been found difficult to implement due to excessive weight and drag penalties of the thermal management system [12]. Palladino et al. show a conceptual fuel cell and TMS architecture including individual component mass predictions. The corresponding thermal management system predictions are based on empirical correlations based on automotive data and heat exchanger technical data sheets. In their study the thermal management system has a mass share of 35 % [13]. Looking at parallel hybrid electric powertrains, Lents concludes on specific heat rejection rates of 1-2 kW heat flow rejected per kilogram TMS weight for the main TMS components. An additional mass penalty of 20 % is recommended to account for TMS components such as coolant pump and piping [14]. Effectively, this yields to a reduction in specific heat rejection rates to 0.83-1.67 kW/kg.
In the present paper the authors propose and analyse a serial cooling system architecture for fuel cell systems. The concept arranges different fuel cells with different operating temperatures in serial from a coolant flow perspective. The objective of this cooling concept is to minimise the additional mass of the thermal management subsystem for a HTPEMFC, and hence increase the power to weight ratio of the combined system.
The paper is organised as follows: In section 2. the serial cooling concept is described in more detail. Following, in section 3. the required fundamentals of HTPEMFCs, the corresponding thermal management systems fundamentals and the calculation logic for the studies analysing the proposed serial cooling concept are briefly described. In section 4. the concept is compared to a baseline cooling system configuration. In addition, several parameter sensitivity studies are carried out and discussed. Finally, the last section summarises the key findings of the presented studies.

2. Concept Description

For aviation applications, next to propulsion system efficiency, propulsion system mass is a key optimisation parameter. The TMS for a fuel cell system is a major contributor to the total system mass, with the liquid coolant mass as a significant contributor within the TMS mass. The main reason is the limited temperature difference available for heat absorption over a fuel cell for longevity and operating stability reasons. A typical value would be only 10 K. The TMS concept discussed in the present paper aims on reducing the required amount of coolant to improve the propulsion systems overall power to weight ratio by increasing the overall temperature difference of the coolant and hence reduce the coolant mass.
For this purpose, the proposed concept puts a number of fuel cell units in serial from a coolant flow perspective. The number of fuel cell units within the studies is varied from 1 to 6. The fuel cell units operate at different temperature levels while maintaining a temperature difference of 10 K over each fuel cell unit. This enables to re-use the coolant for subsequent units and therefore increase the total temperature difference of the coolant over the whole system (see Figure 1) from 10 K to up to 60 K for 6 serial units.
This elevated temperature difference for heat absorption is beneficial for the thermal management system as it leads to a lower coolant mass flow and thus reduced coolant mass while the temperature gradient over the individual fuel cells in each unit are still limited to 10 K.
Due to the different operating temperatures of the cells in each unit the number of cells and efficiencies will vary. There will be a penalty on overall performance and mass from a fuel cell only perspective. The paper aims on evaluating this trade-off between the fuel cell efficiency drawbacks and the thermal management system benefits of the proposed serial cooling concept.
The impact of the different operating temperature levels in the different fuel cell units is only considered with regard to their performance. The impact on other factors such as their individual longevity is not analysed within the scope of this paper.

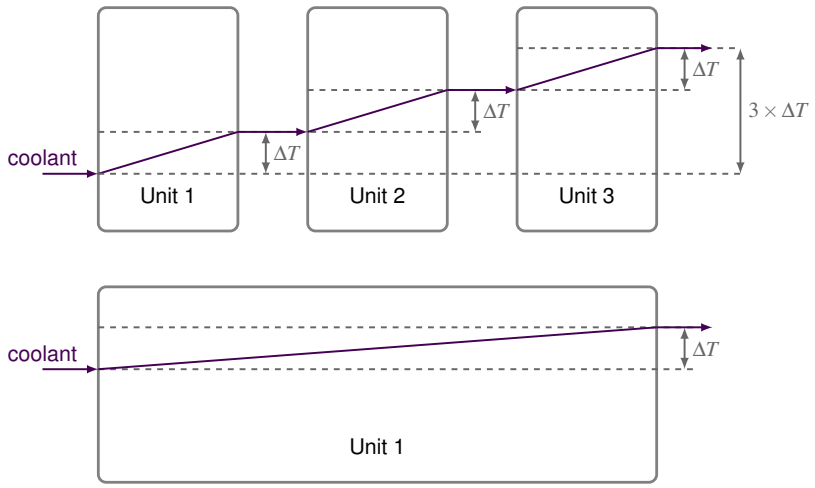

Figure 1 – Re-use of coolant across multiple fuel cell units vs. single fuel cell unit

3. Methodology

3.1 Proton exchange membrane fuel cells

Fuel cells are electrochemical energy converters which produce electricity from the chemical energy of a fuel by an oxidant, usually the oxygen out of the air. There exist several types of fuel cells which mainly differ in the used electrolyte, possible fuels and operating temperature [15]. A very common type is the PEMFC, which has been in the focus of research for fuel cell powered land-based vehicles and small scale portable and stationary power generation in the past decades [16]. Early adaptors have used this fuel cell type in aviation as well for technology demonstrators and small aircraft [17].
The PEMFC class can be subdivided into low and high temperature fuel cells, the first class operating between 50 °C and 90 °C, the latter class from 120 °C up to 200 °C. The LTPEMFCs achieve higher efficiencies and power densities but require a water management system to regulate membrane humidity and to avoid flooding and hence blockage of cell areas. They also present a bigger challenge to the thermal management system due to the low temperature difference to ambient. The advantages of HTPEMFCs are a significantly higher temperature difference to ambient as well as the absence of the need for a water management system and higher tolerance for hydrogen impurities [18]. However, these types of fuel cells have not yet been researched as intensively as LTPEMFCs and therefore are currently not as mature.
For both PEMFC classes the operating temperature is an important parameter for their operating characteristics. Generally, a higher temperature benefits the chemical reactions and increases cell voltage, therefore efficiency and power output of the cell, as can be seen from the polarisation curves for different operating temperatures depicted in Figure 2. On the other hand, e.g. for phosphoric acid-doped polybenzimidazole HTPEMFCs, higher temperatures increase cell degradation due to higher evaporation rates of the phosphoric acid electrolyte and hence reduce lifetime [19]. As mentioned above, these effects are not taken into account in this paper.
The fuel cell model used in this paper is the HTPEMFC model described by Schmelcher [20]. The restriction to a maximum of 6 units with 10 K temperature difference each and the temperature levels within the serial cooling concept stems from the limitations of the model for operating temperatures between 120 °C and 180 °C.
The original model was modified to use an oversizing factor (OF) to determine the design current density and hence power per cell. This factor is defined by Equation 1:

$$OF = \frac{P_{installed}}{P_{required}} \tag{1}$$

Following this oversizing factor definition, a fuel cell unit sized for e.g. 1 kW of required electric power, with an oversizing factor of 2 would hence be able to generate 2 kW of net electric power, when operated at the current density where maximum power per cell is achieved (points marked in Figure 2). But in the design point of 1 kW net power output the cells would run at a lower current

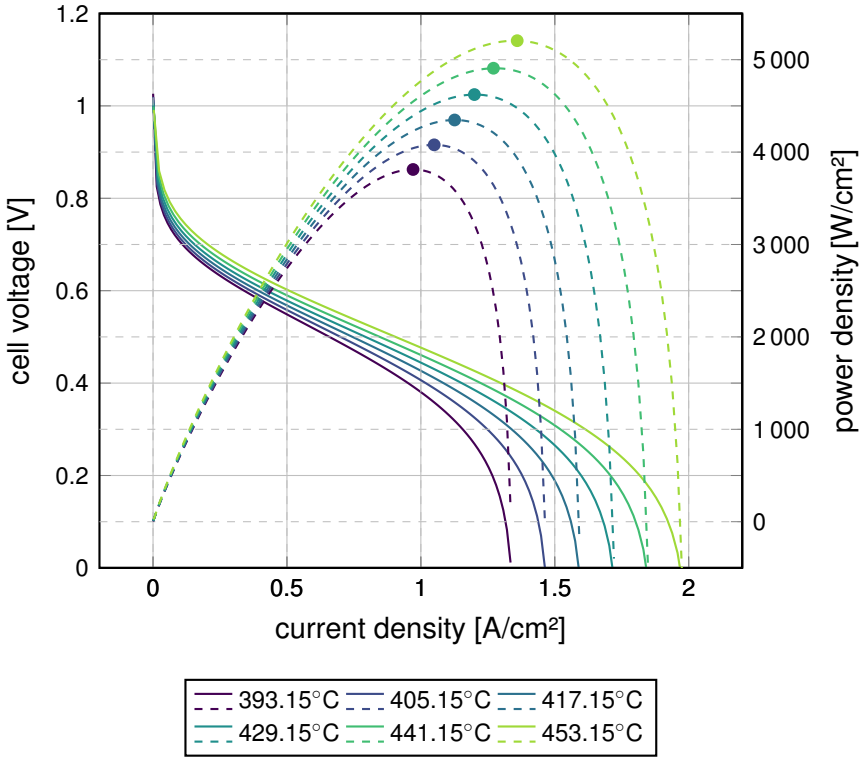

Figure 2 – Operating temperature variation for HTPEMFCs
(cell voltage: solid lines, power density: dashed lines, highest power density marked as dots)

density and hence higher voltage. Thus, the oversizing factor connects the sizing of the fuel cell unit to the maximum power output per cell.
As shown in Figure 2, different cell temperatures change the maximum achievable power density and the corresponding current density. Therefore, two units, sized with the same OF and for the same power requirement but different operating temperatures, operate at different current densities, voltages and therefore efficiencies. As a result, they will have a different number of cells, as the cells in the unit with the higher operating temperature have a higher maximum power density which yields a reduced necessary active cell area to achieve the required power and hence the unit requires less cells.
In the present studies the operating pressure is always held constant at sea level ambient pressure of 1013.25 hPa and a pressure loss over the fuel cells is neglected. Cathode and anode stoichiometry for the fuel cells is consistently set to 2 and 1.2 respectively. Using a fixed active area per cell, the number of cells is determined from the power density in the design operating point and the absolute power requirement.
The mass of the fuel cells is correlated to the active cell area with a value of 1.53 kg/m². The value was derived from a modelled fuel cell stack operating at 180 °C whose mass was calculated with a power to weight ratio of 3 kW/kg, as is currently reached by commercially available LTPEMFCs [21]. Here the assumption is made that HTPEMFCs will achieve this power to weight ratio in the future.

3.2 Thermal management system (TMS)

A simple TMS for a liquid cooled fuel cell consists of several key components as illustrated in Figure 3. For the liquid coolant side the main TMS components are: the coolant itself, a coolant pump as well as a heat exchanger (HEX). To reject the heat to ambient air, an additional air path to the heat exchanger is required which next to an inlet and outlet, requires a fan to ensure sufficient air flow for heat rejection if the mass flow due to ram air effects is insufficient, e.g. during the start of a take-off run of an airplane.

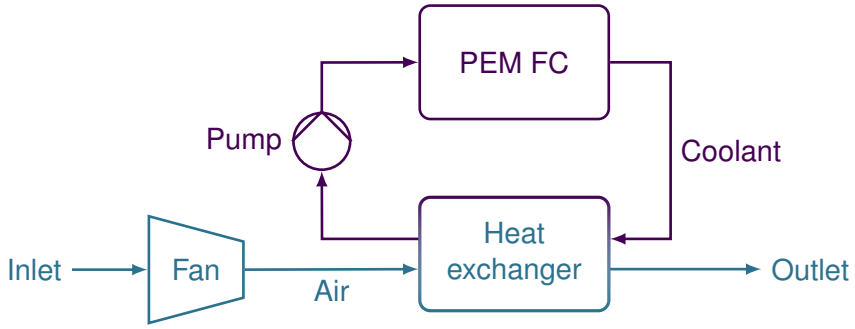

Figure 3 – TMS architecture illustration

3.2.1 Coolant and air mass flows

The size of the TMS is determined by the amount of heat that needs to be rejected. The heat transport equation 2 relates the heat flow $\dot{Q}$ to: a mass flow $\dot{m}$ which absorbs and removes the heat, c_p the heat capacity of the coolant medium and ΔT the temperature difference of the coolant during heat absorption.

$$\dot{Q} = \dot{m} \cdot c_p \cdot \Delta T \tag{2}$$

Equation 2 is applicable for both heat pick-up from the fuel cell via a liquid coolant, as well as for the heat rejection to ambient air. For a given heat flow, limiting the temperature difference for heat pick-up ΔT to small values leads to increasing coolant mass flows $\dot{m}$. Similarly, if ΔT is increased, the required mass flow to reject the heat flow is reduced.

3.2.2 Heat exchanger

The heat rejection to ambient air is carried out via a counterflow heat exchanger (HEX). The sizing of the heat exchanger is done based on the ε-NTU method [22].
For this method, the different fluid sides are characterised by their heat capacity rate for the hot fluid (coolant) and cold fluid (air) respectively (C_{HF} and C_{CF}) which are defined as the product of mass flow $\dot{m}$ and specific heat capacity c_p (Equation 3).

$$C = \dot{m} \cdot c_p \tag{3}$$

The heat capacity ratio R is described by Equation 4 with C_{min} and C_{max} corresponding to the smaller and larger value of the heat capacity rates C_{HF} and C_{CF}.

$$R = \frac{C_{min}}{C_{max}} \tag{4}$$

The effectiveness ε describes the ratio of the actually transferred heat to the maximum possible transferable amount of heat between two fluids (Equation 5).

$$\varepsilon = \frac{q}{q_{max}} = \frac{C_{HF} \cdot (T_{HF_{in}} - T_{HF_{out}})}{C_{min} \cdot (T_{HF_{in}} - T_{CF_{in}})} = \frac{C_{CF} \cdot (T_{CF_{out}} - T_{CF_{in}})}{C_{min} \cdot (T_{HF_{in}} - T_{CF_{in}})} \tag{5}$$

The number of transfer units is given by Equation 6 and defines a relationship between the product of the overall conductance for heat transfer U and the heat transfer area $A_{transfer}$ to the minimum heat capacity rate C_{min} of the two fluids involved in the heat transfer.

$$NTU = \frac{U \cdot A_{transfer}}{C_{min}} \tag{6}$$

The overall conductance for heat transfer U combines the convective heat transfer of both fluid sides (air and coolant) as well as the thermal conductance through the metal. For the purpose of this study, a constant value, driven by the air side of the heat exchanger is implemented. This follows the approach presented by Schmelcher [20].

The relationship between effectiveness ε and number of transfer units NTU for a counterflow heat exchanger is given by Equations 7 and 8 [22, 23]:

$$\varepsilon = \frac{1 - e^{-NTU \cdot (1-R)}}{1 - R \cdot e^{-NTU \cdot (1-R)}} \quad , \tag{7}$$

$$NTU = \frac{1}{(R-1)} \cdot \ln \frac{\varepsilon - 1}{\varepsilon \cdot R - 1} \quad . \tag{8}$$

Within heat exchanger design, increasing the HEX effectiveness ε leads to an increase in air temperature rise across the heat exchanger ΔT_{CF} (see Equation 5). While this reduces the required air mass flow $\dot{m}_{CF}$ (cf. Equation 2) for a given heat flow, it increases the number of transfer units and thus leads to an increased heat transfer area (see Equation 8, 6) and thus heat exchanger mass.
The proposed serial cooling concept increases the temperature difference ΔT_{HF} for heat pick-up of the hot fluid (coolant). As the heat exchanger is designed based on keeping the heat exchanger effectiveness constant the inlet and outlet air temperature of the air remains unchanged. Due to the altered coolant mass flow, the heat capacity ratio R increases which, according to Equation 8, increases the number of transfer units NTU. According to Equation 6, this also leads to an increase in required heat transfer area.

3.2.3 Thermal management system mass calculations

As shown by Equation 9, the mass flow rate provides an estimate of the required coolant mass when multiplied with a coolant circulation time. The circulation time is treated as a study parameter within the presented assessment and will effectively be highly dependent on the chosen propulsion system architecture, applicable flow velocities, pipe lengths, etc. The coolant mass flow rate will also indirectly influence other system component specifications such as the coolant pump and pipes.

$$m_{coolant} = \dot{m}_{coolant} \cdot t_{circ} \tag{9}$$

The heat exchanger mass is estimated based on correlating the calculated heat transfer area $A_{transfer}$ to a thickness of the transfer area d and the density of the heat exchanger material aluminium ρ_{Al} as shown in Equation 10.

$$m_{HEX} = A_{transfer} \cdot d \cdot \rho_{Al} \tag{10}$$

For the thermal management system size, only the heat exchanger and coolant mass are calculated explicitly. Remaining components such as pumps, pipes and a fan are considered by a generic surcharge of 20 % to the calculated mass of the heat exchanger and coolant. This factor is similar to the approach chosen by Lents [14].

3.2.4 Parasitic power loss modelling

The thermal management system has an associated parasitic power loss attributed to the coolant pump and the fan to supply the ambient air to the heat exchanger.
The parasitic power of the coolant pump is neglected for the presented studies as the pump power will be at a lower order of magnitude compared to the fan system due to the differences in compression for compressible and incompressible fluids [14, 24].
For the fan, the temperature rise during compression to overcome the pressure losses in the air path, as given in Equation 11, is calculated assuming an isentropic change of state with a constant isentropic efficiency η_{is}, inlet air temperature $T_{fan_{in}}$ and fan pressure ratio Π. Hereby, the pressure ratio needs to ensure that all system pressure losses, such as the pressure loss over the HEX, are compensated. κ refers to the heat capacity ratio of air.

$$\Delta T_{fan} = \frac{1}{\eta_{is}} \cdot T_{fan_{in}} \cdot (\Pi^{\frac{\kappa-1}{\kappa}} - 1) \tag{11}$$

As shown in Equation 12, the required work is proportional to the mass flow rate $\dot{m}_{CF}$, an assumed constant specific heat capacity of air c_p and the temperature rise ΔT_{fan}. This is converted to an

electrical power via an additional electric efficiency η_{el} accounting for an electric motor driving the shaft of the fan.

$$P_{fan} = \frac{1}{\eta_{el}} \cdot \dot{m}_{CF} \cdot c_p \cdot \Delta T_{fan} \tag{12}$$

3.2.5 Implications of HEX design on parasitic power loss

Varying the heat exchanger effectiveness leads to a trade-off between heat transfer area and required air mass flow. While the heat transfer area influences the heat exchanger size and mass, the air mass flow affects the parasitic power. The air mass flow and therefore parasitic power decrease with increasing heat exchanger effectiveness. This results in less additional fuel cells to compensate for this parasitic power loss. At the same time a larger heat transfer area is required which increases the heat exchanger mass.

3.3 Calculation logic

A sizing methodology focusing on waste heat is used to size the fuel cell units and TMS for the proposed serial cooling concept. The implemented calculation logic is displayed in Figure 4.

Based on Equation 2, when the coolant flow is re-used and the temperature difference across each unit is kept constant, all systems are required to reject the same amount of waste heat $\dot{Q}_n$. This implies the assumption of a constant specific heat capacity of the coolant across the operating range. The individual fuel cell units, operating at different temperatures T_n, are therefore sized for a waste heat and not a power output. This is done by an internal iteration loop for each unit in which the number of cells is determined. The electric power of each unit is hence only available as a result.

From the total heat flow of all units $\dot{Q}_{total}$ and the total temperature difference over all fuel cell units the TMS is sized and the parasitic power of the fan is calculated.

As the whole fuel cell system is sized for a net electric power output P_{net}, the calculation logic adds an outer iteration loop which takes these parasitic power losses of the TMS P_{TMS} into account and iterates for the net electric power output P_{net}.

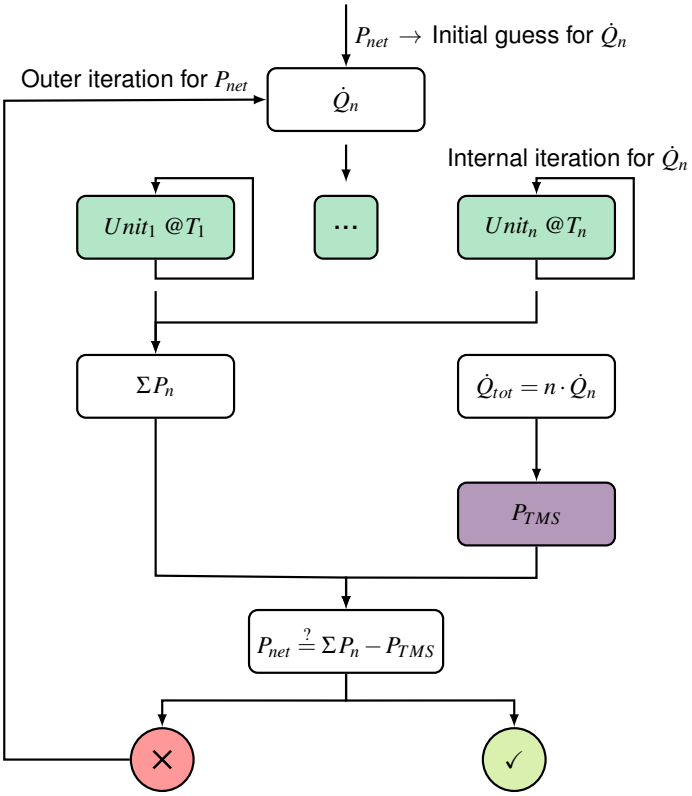

Figure 4 – Illustration of calculation logic for waste heat sizing approach

Key metrics for the serial cooling concept are fuel cell system mass, thermal management system mass, combined system mass as well as corresponding power to weight ratio and system efficiency. Power to weight ratio is defined as the net electric power divided by the total system mass, while the system efficiency references the net electric power to the hydrogen mass flow and the lower heating value of hydrogen.

4. Studies

The total system mass of a fuel cell power system is generally very sensitive to the net power requirement, the selected fuel cell oversizing factor, heat exchanger effectiveness and coolant circulation time. Within the presented studies, if not explicitly mentioned as varied, the values listed in Table 1 are used.

Parameter	Symbol	Unit	Value
Net Power	P_{net}	[W]	1 000 000
Fuel cell oversizing factor	OF	[-]	1.5
HEX effectiveness	ε	[-]	0.6
Coolant circulation time	t_{circ}	[s]	10

Table 1 – Key parameter assumptions for studies

All calculations were carried out for a static ISA+15 K case at sea level ambient conditions and for a liquid cooling system with a generic coolant with a specific heat capacity of c_p=3 000 J/kgK. Future coolant capabilities for HTPEMFC applications are still under development. Experimental tests in the past have been carried out with technical heat transfer fluids (e.g. Supra et al. [25]) which only provide a specific heat capacity of c_p=2 000-2 500 J/kgK. Higher specific heat capacity values can be attributed to LTPEMFC coolants and mixtures such as Ethylene-Glycol-Water (c_p up to 3 500 J/kgK) which have limited operating temperature capability compared to HTPEMFC operating conditions.

4.1 Temperature difference ΔT for heat pick-up

The baseline case uses a temperature difference for heat pick-up ΔT of 10 K with a corresponding average fuel cell operating temperature of 175 °C. The coolant enters the fuel cells at 170 °C and exits at 180 °C. This range is increased to up to 60 K over 6 fuel cell units within the studies. The fuel cell units operating temperature are always chosen to be as high as possible to achieve highest efficiencies. For more than one fuel cell unit the average operating temperatures drop depending on the number of units by 10 K with each unit, starting at 175 °C. For the maximum of 6 units the average fuel cell unit operating temperatures are 125 °C, 135 °C, 145 °C, 155 °C, 165 °C and 175 °C. The coolant entry temperature is reduced to a minimum of 120 °C while the exit temperature remains at 180 °C.

Figure 5a illustrates the reduction of coolant mass at the expense of fuel cell and heat exchanger mass with an increase of serial fuel cell units and hence overall coolant ΔT. A total system mass reduction is present as long as the coolant mass reduction exceeds the incurring mass penalty for fuel cell and heat exchanger.

The lowest system mass is also characterised by the peak in power to weight ratio as shown in Figure 5b, as the net power output for all cases is the same. An absolute maximum is reached at a coolant temperature difference of 40 K or 4 units in serial. In the present study the largest stepwise power to weight improvement is already achieved when increasing the number of serial fuel cell units from one to two. With the given set of assumptions, the efficiency penalty is small as shown by the nearly constant η_{Sys} in Figure 5b and thus this study already shows the general viability of the concept.

Tabulated results for a more detailed comparison for the baseline case against the identified best case of ΔT=40 K are provided in Table 2 with the component mass breakdown additionally illustrated in Figure 6.

When applying the serial cooling concept under the mentioned circumstances with 4 units, the total system efficiency is reduced by 0.9 %, due to the lower efficiencies of the fuel cell units operating at

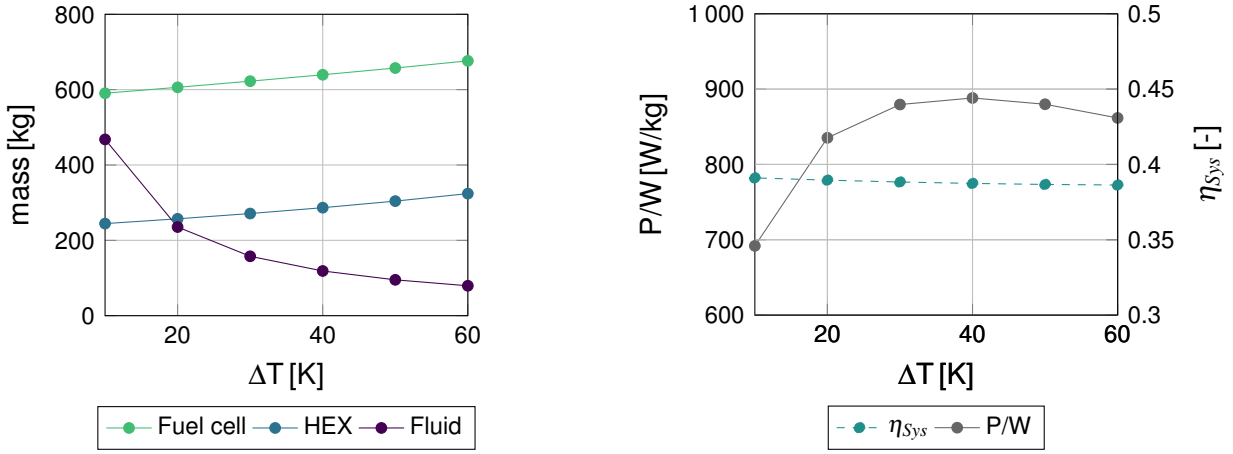

(a) Mass vs. coolant ΔT

(b) System P/W and efficiency η_{Sys} vs. coolant ΔT

Figure 5 – Coolant temperature difference study results

Parameter	**Unit**	**ΔT=10 K**	**ΔT=40 K**	**Relative Change [%]**
Heat flow	[W]	1 403 780	1 423 971	+1.4
System efficiency	[%]	39.1	38.7	-0.9
Coolant mass flow	[kg/s]	46.8	11.9	-74.6
Air mass flow	[kg/s]	16.5	16.7	+1.4
TMS power required	[W]	153 682	155 893	+1.4
Fuel cell mass	[kg]	590.5	639.5	+8.3
Coolant mass	[kg]	467.9	118.7	-74.6
Heat exchanger mass	[kg]	244.4	286.7	+17.3
TMS mass surcharge (20%)	[kg]	142.5	81.1	-43.1
TMS total mass	[kg]	854.8	486.4	-43.1
Total system mass	[kg]	1 445.3	1 125.9	-22.1
Power to weight ratio	[W/kg]	691.9	888.2	+28.4
Specific heat rejection	[kW/kg]	1.64	2.93	+78.6

Table 2 – Results comparison of 10 K and 40 K temperature difference for coolant heat pick-up

lower temperatures.

On the other hand, a reduction of the coolant mass flow by slightly less than a factor of 4 can be observed. A factor of 4 (or -75 %), which one could expect due to a comparison of 4 units vs. 1 unit, is not exactly met due to the slightly lower fuel cell efficiency of the colder cells. This yields a slightly higher total heat flow (+1.4 %) and therefore a higher than intuitively expected required coolant mass flow. The reduced coolant mass flow in combination with the assumed circulation time still leads to a significant reduction of required coolant mass by 74.6 %.

With the lower efficiency and therefore increase waste heat the air flow required to reject the heat to ambient air is also increased by 1.4 %. This directly correlates to an increase in parasitic power of the thermal management system by again 1.4 %.

As the HEX effectiveness ε is held constant with the increase in heat flow and temperature difference of the hot fluid, the required heat transfer area $A_{transfer}$ of the HEX increases. In consequence the mass of the heat exchanger increases by 17.3 %. The change in operating temperature, and hence efficiency and maximum power density of the cells, also has a notable impact on the number of cells within the fuel cell units and thus total fuel cell mass, which increases by 8.3 %.

Nonetheless, for the combined system of fuel cell units and TMS a mass reduction of 22.1 % is achieved which corresponds to a power to weight ratio increase by 28.4 %. The calculated specific heat rejection increases by 78.6 % from 1.64 kW/kg to 2.93 kW/kg.

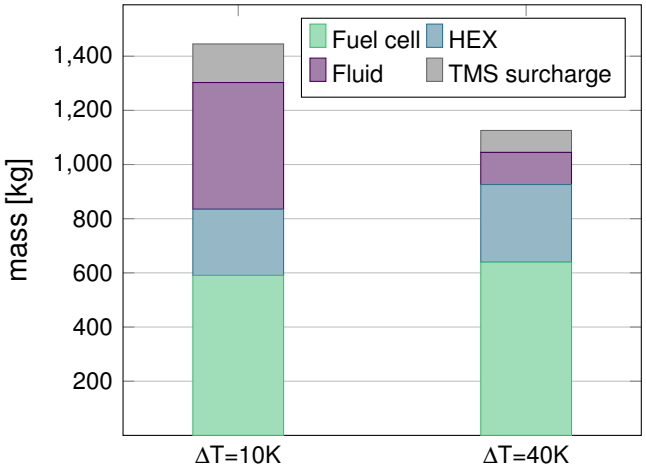

Figure 6 – Component mass comparison for varied temperature differences ΔT for heat pick-up

4.2 Heat exchanger (HEX) effectiveness ε

In the prior study on temperature difference ΔT the heat exchanger was always designed with the same heat exchanger effectiveness ε of 0.6. Changing the effectiveness value to 0.4 or 0.8 shows significant impact on the individual mass contributors coolant, heat exchanger and fuel cell units (see Figure 7a). An increase in heat exchanger effectiveness leads to a reduction in fuel cell mass at the expense of a larger heat exchanger. As previously described in section 3.2, the chosen heat exchanger effectiveness alters the required air mass flow as more air is required to reject the same amount of heat for lower effectiveness values. Since the required air mass flow is coupled to the overall parasitic power of the thermal management system by the fan, a higher parasitic power of the TMS results in an increase in the number of fuel cells within the fuel cell units to provide the same net power. This results in an avalanche effect, as more heat has to be rejected which in consequence requires more air mass flow and yields a higher TMS parasitic power for which more fuel cells are needed to compensate which again increase the total heat flow. This is reflected in a reduced system efficiency which is illustrated in Figure 7b next to the power to weight ratio. A peak of the power to weight ratio is observed for a temperature difference of the coolant of 30 K or 40 K. The peak achievable power to weight ratio depends on the chosen heat exchanger effectiveness. The calculations with 0.6 yielded the highest peak power-to-weight ratios while 0.4 and 0.8 resulted in lower values.

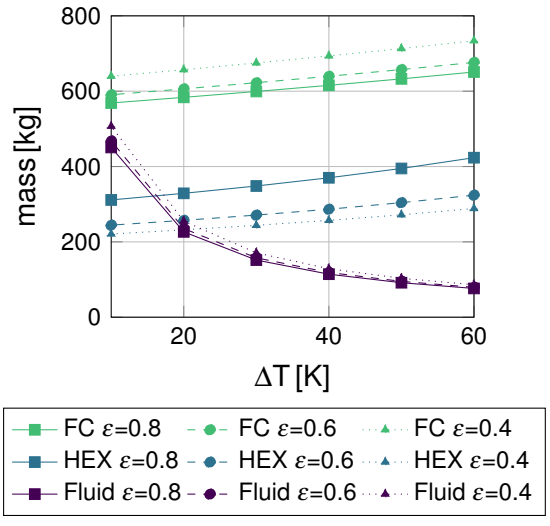

(a) Mass vs. coolant ΔT

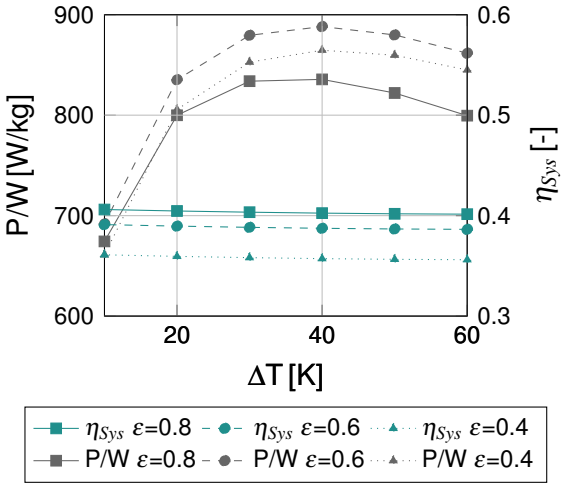

(b) System P/W and efficiency η_{Sys} vs. coolant ΔT

Figure 7 – Heat exchanger effectiveness study results

From a performance perspective, the total fuel cell system efficiency increases with higher heat exchanger effectiveness values as less oversizing of the system is required to supply the required parasitic power to move the air as shown in Figure 7b. Therefore values around 0.6 up to 0.8 seem best under these conditions.

4.3 Oversizing Factor OF

A key parameter for the fuel cell units is their oversizing factor OF as described in section 3.1. Values between 1.25 and 2.0 are analysed. While increasing the factor increases fuel cell mass (Figure 8a) - at the same time the efficiency increases (Figure 8b) and hence the heat generated by the fuel cell units is reduced and the required thermal management system mass follows this trend.
With regard to the power to weight ratio (Figure 8b), the peak at 40 K is visible for lower oversizing factors of 1.25 to 1.5. With increasing oversizing factor, the peak moves to a temperature difference of 30 K due to the generally lower TMS mass (see Figure 8a) due to the higher efficiency. The absolute peak power to weight ratio values are decreasing due to the significantly increasing fuel cell mass. The highest power to weight value was reached for 40 K temperature difference and an OF of 1.25 at approximately 900 W/kg at the cost of a low efficiency of only about 35 %.

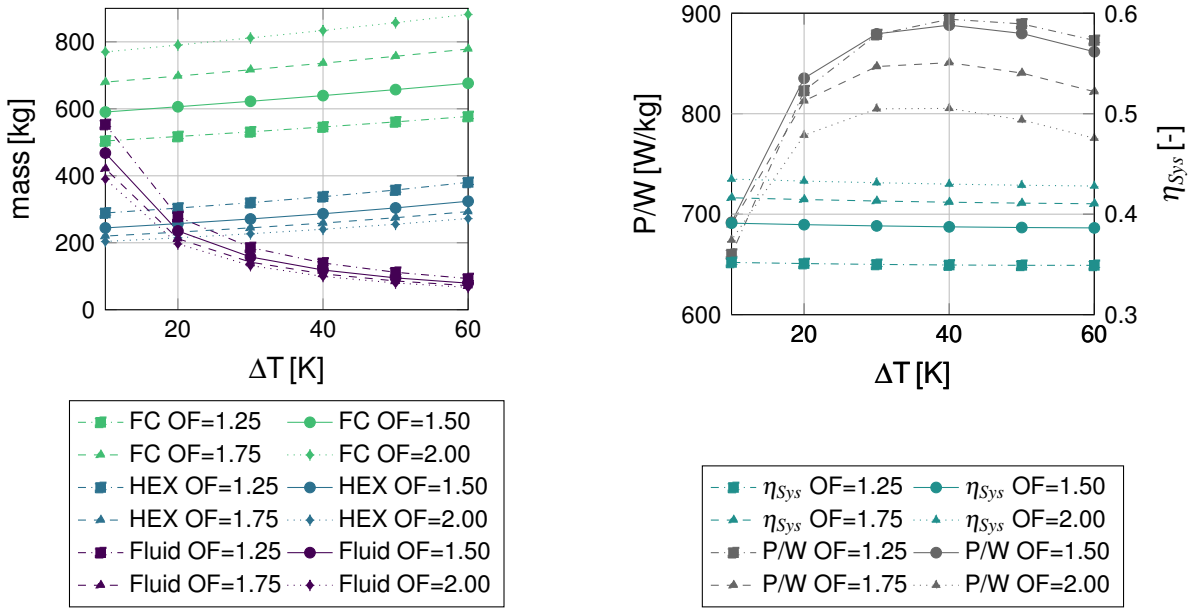

(a) Mass vs. coolant ΔT

(b) System P/W and efficiency η_{Sys} vs. coolant ΔT

Figure 8 – Fuel cell oversizing factor study results

4.4 Combination of contributing factors: HEX effectiveness ε and oversizing factor OF

Both, fuel cell oversizing factor OF and HEX effectiveness ε studies indicate a minimum mass potential for a temperature difference ΔT across the TMS of 30 K or 40 K while showing sensitivity to the absolute parameter value.
Therefore, a combined study looking at HEX effectiveness and fuel cell oversizing factor for a temperature difference across the TMS of ΔT=10 K (conventional, no serial cooling concept) and ΔT=40 K is carried out. Figure 9 shows the results of the study for ΔT=40 K.
The total system mass is depicted in Figure 9a for all different HEX effectiveness and oversizing factors as a contour plot. Additionally, the point for the HEX effectiveness and oversizing factor for the reference case (ε=0.6, OF=1.5) and the point of the lowest mass are marked. They show that the selected reference case does not represent the best combination when looking solely at system mass but does not deviate much either. The region with the lowest masses is located between oversizing factors of 1.3 and 1.55 and HEX effectiveness values between 0.4 and 0.75.
Figure 9b shows the total system efficiencies for the same parameter range, also as a contour plot. The efficiency values rise with increasing oversizing factor and HEX effectiveness with higher sensi-

tivity to the oversizing factor. Again the reference case combination and the combination that yielded the lowest mass are marked. While the reference combination was not optimal in terms of total system mass, it yields a higher total system efficiency.

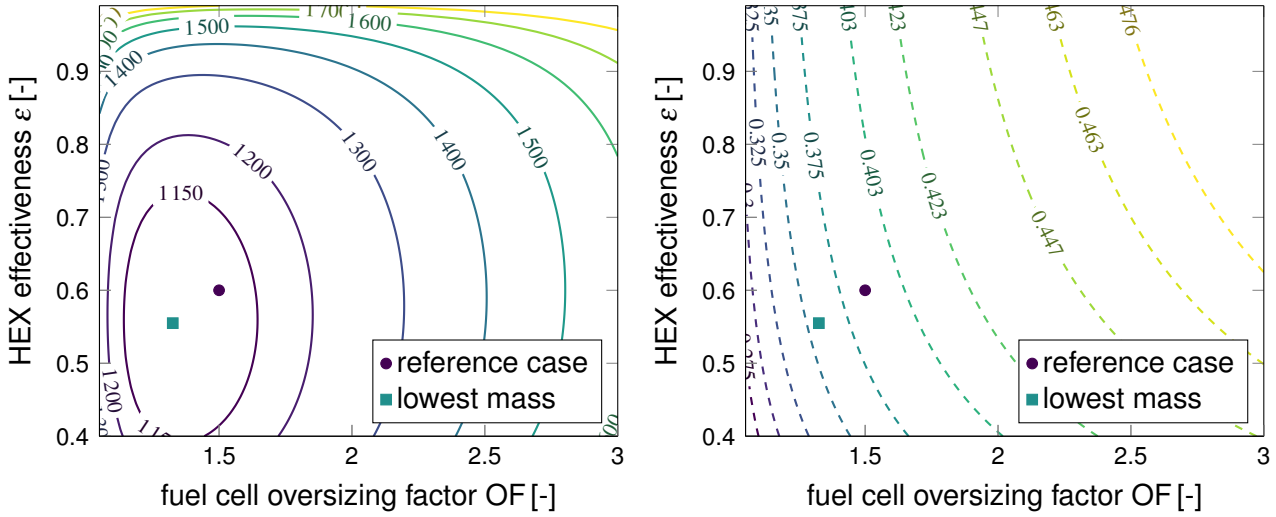

(a) System mass for ΔT=40 K

(b) System efficiency for ΔT=40 K

Figure 9 – Combined HEX effectiveness and oversizing factor study results for ΔT=40 K

The shape of the mass and efficiency contour lines allow for optimisation of oversizing factor and HEX effectiveness to get as high as possible efficiency for a given mass. Figure 10 shows both contour plots on top of each other. Additionally marked to reference and lowest mass combination are now the points on the mass contour lines that yield the highest efficiencies. If these points were to be connected, a relation where one could trade mass vs. efficiency could be established for such a system.

As an example, such a trade-off was carried out with respect to the minimum mass case for 10 K temperature difference, the results are listed in Table 3. The minimum mass for 10 K temperature difference is 1 441 kg at an efficiency of 40.5 %. The 40 K temperature difference case has a mass minimum of 1 110 kg, corresponding to a mass decrease of 23 %, but for this point the efficiency is reduced by nearly 5 percentage points to only 35.8 %.

If the mass reduction is not the primary criterion, the serial cooling concept can be used to maximise system efficiency. A point yielding a mass close to the 1 441 kg of the 10 K temperature difference case on the line of best combinations from Figure 10 can be found, yielding about 1 443 kg but an efficiency of 48.5 %, a significant increase of 8 percentage points.

Parameter	**Symbol**	**Unit**	**ΔT=10 K**	**ΔT=40 K**	
			min mass	min mass	max efficiency @ min mass(ΔT=10K)
heat exchanger effectiveness	ε	[-]	0.62	0.55	0.78
fuel cell oversizing factor	OF	[-]	1.60	1.33	2.53
system mass	m_{total}	[kg]	1 441.1	1 110.3	1 443.8
system efficiency	η	[%]	40.5	35.8	48.5
power to weight ratio	P/W	[W/kg]	693.9	900.7	692.6
mass change to ΔT=10 K	Δm	[%]	N/A	-23.0	+0.2

Table 3 – Results combined HEX effectiveness and fuel cell oversizing factor optimisation

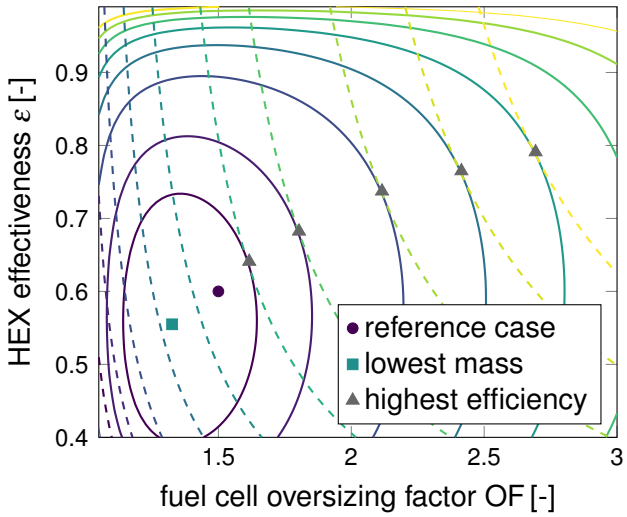

Figure 10 – Combined system mass and system efficiency contour plot for ΔT=40 K

4.5 Coolant circulation time t_{circ}

The coolant required to absorb the waste heat needs to be circulated from the fuel cell units to the heat exchanger. Depending on the system architecture this will lead to different coolant circulation times as a distributed system with independent propulsion units might work with shorter pipe lengths and thus quicker circulation of the coolant compared to a centralised system with longer pipe routings. In this study the coolant circulation time is varied from 5 to 20 seconds. At flow velocities of the coolant of 1-2 m/s, this would provide a potential routing range of 5 to 20 m or 10 to 40 m respectively. For a system with a short circulation time the coolant mass is already lower and a smaller share of the TMS total mass. Therefore, the benefits of the proposed concept are expected to be lower. The corresponding changes in coolant mass are shown in Figure 11a.

Figure 11b illustrates the relative mass change for the different coolant temperature differences and circulation times compared to the baseline system. For very quickly circulating systems, the benefit of the serial cooling concept w.r.t. total system mass is limited to approx. 8 %, while with increasing circulation times the benefit increases significantly to 18 % for 10 s, 27 % for 15 s and 34 % for 20 s circulation time. The sensitivity to coolant circulation time t_{circ} similarly affects the achievable power to weight ratio (Figure 11c). With regard to the relative change of the power to weight ratio compared to the corresponding baseline cases of ΔT=10K, systems with increasing circulation time show higher improvement potentials of the power to weight ratio.

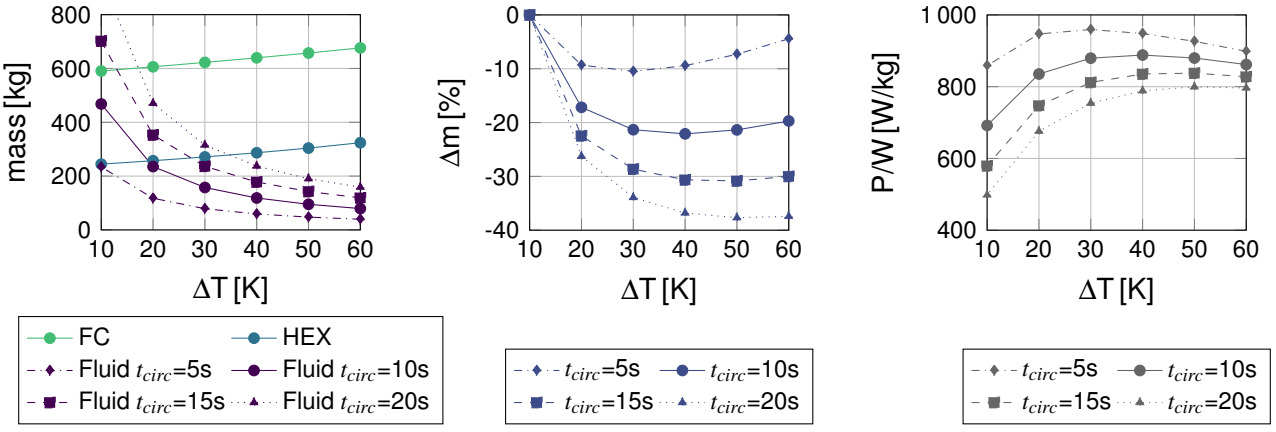

(a) Mass vs. coolant ΔT

(b) Mass reduction vs. coolant ΔT

(c) System P/W vs. coolant ΔT

Figure 11 – Circulation time study results

4.6 Fuel cell weight factor

Next to the circulation time, the fuel cell weight factor is a key parameter limiting the potential mass reductions. From a long term development perspective it is assumed, that the fuel cell weight is reduced and optimised as much as possible. A study has been carried out varying the fuel cell weight factor from 1.0 kg/m² to 3.5 kg/m².

The associated impact on fuel cell weight is illustrated in Figure 12a. Next to the increase in baseline fuel cell mass (for ΔT=10 K), the associated fuel cell mass increase with increasing ΔT is also higher with increased fuel cell weight factor.

Figure 12b illustrates the relative mass change compared to the baseline system. While the reduction potential is limited to 12 % for the highest fuel cell weight factor of 3.5 kg/m², improvements of more than 20 % can be achieved for lighter systems.

The sensitivity to the fuel cell weight also affects the achievable power to weight ratio (Figure 12c). An increased fuel cell weight factor, negatively impacts the proposed solution as the penalty incurring from the additional fuel cells due to running them at lower temperatures is more significant as for lighter systems. In addition, the relative share of TMS mass within the whole system is smaller to begin with.

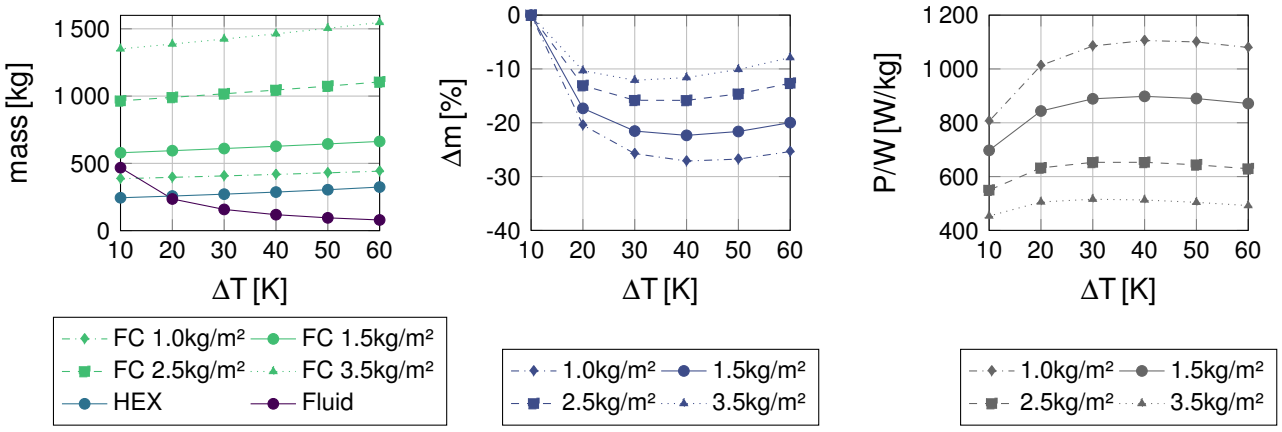

(a) Mass vs. coolant ΔT

(b) Mass reduction vs. coolant ΔT

(c) System P/W vs. coolant ΔT

Figure 12 – Fuel cell area to weight scaling study results

5. Summary

A serial cooling concept for HTPEMFCs is introduced and assessed for its effects on component and total masses as well as system efficiency. The coolant mass decreases significantly for the serial cooling concept, at the same time heat exchanger and fuel cell mass increase. Nonetheless, the concept shows total mass reductions of over 20 % with minimal system efficiency drawbacks in a first assessment, without further optimisation.

Parameter studies on key parameters, such as heat exchanger effectiveness, fuel cell oversizing factor, coolant circulation time and fuel cell weight factor are carried out. One major finding from these studies is that a maximum of four fuel cell units in serial usually yielded the best performance. In the region of two to four fuel cell units the mass reduction of the coolant strongly outweighs the mass increase of heat exchanger and fuel cell.

In a combined parameter study of HEX effectiveness and fuel cell oversizing factor the influence on system mass and efficiency are analysed and visualised. The study shows, an optimisation solely for mass can have significant drawbacks in terms of efficiency, and there exist certain parameter combinations that give best results in terms of mass and efficiency. Furthermore the potential to use the concept to solely increase system efficiency was demonstrated. A higher system efficiency leads to less required fuel and thus less fuel mass.

The identified mass reduction potential of over 20 % is applicable for systems with circulation times of 10 s at the investigated fuel cell weight factor. Even higher reductions can be achieved for systems with longer circulation times. At application level, e.g. for fuel cell powered aircraft, this corresponds to a lower overall system mass reduction potential for decentralised fuel cell unit architectures such as distributed propulsion systems. A higher overall system mass reduction potential is available for more centralised architectures with a fuselage integrated fuel cell system.

6. Contact Author Email Address

Mailto: antje.link@dlr.de

7. Copyright Statement

References

[1] European Commission. *Flightpath 2050. Europe's vision for aviation; Maintaining global leadership and serving society's needs; Report of the High-Level Group on Aviation Research*. 2nd edition, Publications Office of the European Union, 2012.

[2] Smedberg A, Norberg I and Oja S. *Electric aviation 2021: Technology overview*. `https://www.kvarken.org/wp-content/uploads/2021/06/Electric_aviation_2021_technology_overview.pdf`, 2021, retrieved 08.02.2022.

[3] German Aerospace Center (DLR). *Zero Emission Aviation: German Aviation Research White Paper*. `https://www.dlr.de/content/en/downloads/publications/brochures/2020/white-paper-dlr-bdli-zero-2020-en.pdf?__blob=publicationFile&v=4`, 2020.

[4] McKinsey & Company. *Hydrogen-powered aviation: A fact-based study of hydrogen technology, economics and climate impact by 2050*. 1st edition, Publications Office of the European Union, 2020.

[5] Deutsches Zentrum für Luft- und Raumfahrt e.V.. *Auf dem Weg zu einer emissionsfreien Luftfahrt - Luftfahrtstrategie des DLR zum European Deal*. 2021.

[6] Sahoo S, Zhao X and Kyprianidis K. A review of concepts, benefits, and challenges for future electrical propulsion-based aircraft. *Aerospace*, Vol. 7, No. 4, Article No. 44, 2020.

[7] Dicks A and Rand D A J. *Fuel cell systems explained*. 3rd edition, Wiley, 2018.

[8] Bargal M H S, Abdelkareem M A A, Tao Q, Li J, Shi, J and Wang, Y. Liquid cooling techniques in proton exchange membrane fuel cell stacks: A detailed survey. *Alexandria Engineering Journal*, Vol. 59, No. 2, pp 635–655, 2020.

[9] Zhang G and Kandlikar S G. A critical review of cooling techniques in proton exchange membrane fuel cell stacks. *International Journal of Hydrogen Energy*, Vol. 37, No. 3, pp 2412–2429, 2012.

[10] Ravishankar S and Arul Prakash K. Numerical studies on thermal performance of novel cooling plate designs in polymer electrolyte membrane fuel cell stacks. *Applied Thermal Engineering*, Vol. 66, No. 1-2, pp 239–251, 2014.

[11] Sasiwimonrit K and Chang W-C. Thermal management of high temperature polymer electrolyte membrane fuel cells by using flattened heat pipes. *Thermal Science*, Vol. 25, No. 4 Part A, pp 2411-2423, 2021.

[12] Waddington E, Merret J M and Ansell P J. Impact of LH2 fuel cell-electric propulsion on aircraft configuration and integration. *AIAA AVIATION 2021 FORUM*, virtual, Paper No. AIAA 2021-2409, 2021.

[13] Palladino V, Jordan A, Bartoli N, Schmollgruber P, Pommier-Budinger V and Benard E. Preliminary studies of a regional aircraft with hydrogen-based hybrid propulsion. *AIAA AVIATION 2021 FORUM*, virtual, Paper No. AIAA 2021-2411, 2021.

[14] Lents C E. Impact of weight, drag and power demand on aircraft energy consumption. *AIAA Propulsion and Energy 2021 Forum*, virtual, Paper No. AIAA 2021-3322, 2021.

[15] Hoogers G. *Fuel cell technology handbook*. 1st edition, CRC Press, 2003.

[16] Wang Y, Ruiz Diaz D F, Chen K S, Wang Z and Adroher, X C. Materials, technological status, and fundamentals of PEM fuel cells – A review. *Materials Today*, Vol. 32, pp 178–203, 2020.

[17] Deutsches Zentrum für Luft- und Raumfahrt e.V.. *Zero-emission air transport - first flight of four-seat passenger aircraft Hy4*. https://www.dlr.de/content/en/articles/news/2016/20160929_zero-emission-air-transport-first-flight-of-four-seat-passenger-aircraft-hy4_19469.html, 2016, retrieved 20.12.2021.

[18] Rosli R E, Sulong A B, Daud W R W, Zulkifley M A, Husaini T, Rosli M I, Majlan E H and Haque M A. A review of high-temperature proton exchange membrane fuel cell (HT-PEMFC) system. *International Journal of Hydrogen Energy*, Vol. 42, No. 14, pp 9293–9314, 2017.

[19] Waller M G, Walluk M R and Trabold T A. Performance of high temperature PEM fuel cell materials. Part 1: Effects of temperature, pressure and anode dilution. *International Journal of Hydrogen Energy*, Vol. 41, No. 4, pp 2944–2954, 2016.

[20] Schmelcher M. *Potenzialbewertung eines mit Wasserstoff betriebenen Brennstoffzellen-Antriebssystems für verschiedene Flugzeugklassen: Masterarbeit*, 2021.

[21] PowerCell Sweden AB. *PowerCellution P Stack Datasheet*. https://www.datocms-assets.com/36080/1636022110-p-stack-v-221.pdf, Version 221, retrieved 08.02.2022.

[22] Kays W M and London A L. *Compact Heat Exchangers*, 3rd edition, Krieger Publishing Company, 1998.

[23] Karwa R. *Heat and Mass Transfer*. 2nd edition, Springer, 2020.

[24] Kellermann H, Lüdemann M, Pohl M and Hornung M. Design and optimization of ram air–based thermal management systems for hybrid-electric aircraft. *Aerospace*, Vol. 8, No. 3, Article no. 3, 2020.

[25] Supra J, Janßen H, Lehnert W and Stolten D. Temperature distribution in a liquid-cooled HT-PEFC stack. *International Journal of Hydrogen Energy*, Vol. 38, No. 4, pp 1943–1951, 2013.